Nanoscale

COMMUNICATION

View Article Online
View Journal | View Issue

Cite this: *Nanoscale*, 2023, **15**, 8148

Received 11th January 2023,
Accepted 9th April 2023

DOI: 10.1039/d3nr00171g

rsc.li/nanoscale

Tuning the enzyme-like activity of peptide–nanoparticle conjugates with amino acid sequences

Xiaojin Zhang, Yichuan Wang, Yu Dai * and Fan Xia *

We constructed peptide–nanoparticle conjugates (AuNP@CDs-Azo-peptide) by self-assembly of cyclodextrin capped gold nanoparticles (AuNP@CDs) and azobenzene terminated peptide (Azo-peptide) through host–guest interactions. AuNP@CDs-Azo-peptide shows hydrolase-like activity, which is tuned by amino acid sequences.

Introduction

Natural enzymes have some disadvantages, such as poor stability, denaturation and poor tolerance to pH, temperature, and solvent.[1] Therefore, it is of great significance to develop artificial enzymes to overcome the disadvantages of natural enzymes. Artificial enzymes are designed reasonably according to the structure and function of natural enzymes.[2] Through exploration by scientific researchers, artificial enzymes that can mimic the catalytic activity of natural enzymes have been constantly reported.[3] Among them, peptide-based artificial enzymes have similar structures and catalytic mechanisms to natural enzymes.[4] Peptide-based artificial enzymes have many significant advantages.[5] (1) The design of the amino acid sequence can directly refer to the catalytic site of natural enzymes, because most natural enzymes are proteins composed of amino acids. (2) The catalytic site with a specific structure and function can be easily embedded into the peptide; thus the structure design is facile. (3) Peptides composed of amino acids have good biocompatibility and can catalyze reactions under relatively mild conditions.

The amino acids at the catalytic site of natural enzymes mainly include histidine, aspartic acid, arginine and serine.[6] For example, the catalytic triad of serine protease consists of serine, histidine and aspartic acid.[7] The imidazole group in histidine attacks the carbonyl carbon atom in the peptide bond. The imidazole group in histidine is very important for the efficient catalysis of natural enzymes.[8] The early peptide-based artificial enzyme was made to add histidine into the peptide, which successfully mimicked the catalytic activity of esterase.[9] It has been reported that the catalytic activity of the artificial enzyme can be improved by increasing the density of catalytic sites.[10] Zhao *et al.* reported that the nanofiber structure formed by the self-assembly of a peptide effectively improves the density of histidine.[11] The study of peptide-based artificial enzymes is of great significance for exploring the origin of natural enzymes and understanding the mechanism of natural enzymes.[12] The design of peptide-based artificial enzymes with tunable catalytic activity remains a challenge.

Here, we designed peptide–nanoparticle conjugates with different positions of histidine in the peptide (Scheme 1). Cyclodextrin capped gold nanoparticles (AuNP@CDs)[13] and azobenzene terminated peptide (Azo-peptide) self-assemble to form peptide–nanoparticle conjugates (AuNP@CDs-Azo-peptide) through host–guest interactions. AuNP@CDs-Azo-peptide shows hydrolase-like activity. Because of the different positions of histidine in the peptide, their catalytic activities are also different. The Michaelis–Menten constant, reaction rate constant and activation energy of 4-nitrophenyl acetate (4-NPA) hydrolysis catalyzed by AuNP@CDs-Azo-peptide were calculated. Azobenzene has the characteristics of photoisomerization, and AuNP@CDs-Azo-peptide disassembles/assembles with UV/visible light irradiation. AuNP@CDs-Azo-peptide catalyzes the hydrolysis of 4-NPA to 4-nitrophenol (4-NP), while AuNP@CDs further catalyze the reduction of 4-NP to 4-aminophenol (4-AP). This work provides a facile method for constructing a photo-regulated artificial enzyme, and tuning the catalytic activity of artificial enzymes with amino acid sequences.

Experimental

AuNP@CDs-Azo-peptide was prepared by mixing AuNP@CDs (0.36 mg mL^{-1}, 20 μL) with Azo-peptide (0.9 mg mL^{-1}, 30 μL), followed by incubating in a shaker at room temperature for

State Key Laboratory of Biogeology Environmental Geology, Engineering Research Center of Nano-Geomaterials of Ministry of Education, Faculty of Materials Science and Chemistry, China University of Geosciences, Wuhan 430074, China.
E-mail: yudai@cug.edu.cn, xiafan@cug.edu.cn

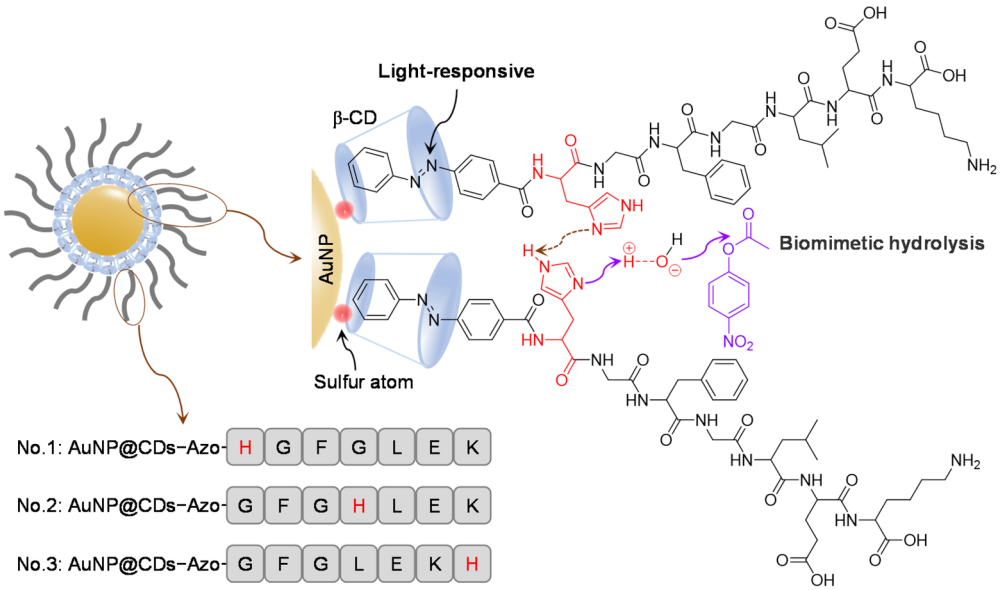

Scheme 1 Structure of AuNP@CDs-Azo-peptide. AuNP@CDs was synthesized by a one-step method, forming stable Au–S bonds.[14] Azo-peptide was anchored onto the surface of AuNP@CDs through host–guest interactions. By changing the amino acid sequences, the catalytic site, imidazole, at different positions was designed. Azobenzene is a classical photo-responsive molecule.[15] Deprotonation from neighboring histidine facilitates proton splitting from water, thus promoting nucleophilic attack on the substrate.

1 h. The mixture was centrifuged (10 000 rpm, 20 min) to remove the residual Azo-peptide. The precipitate was dispersed in ultrapure water (30 μL).

AuNP@CDs-Azo-peptide (4 μL) was added into the 4-NPA solution. The total volume of solution was 200 μL. The final concentration of 4-NPA was 0.12 mM. The absorbance of the hydrolysate 4-NP was recorded by UV-Vis spectroscopy (UV-2600, Shimadzu) to calculate the reaction rate constant (k). The reaction rate constants of catalytic hydrolysis at different temperatures were obtained to calculate the activation energy (E_a). The values of the absorption peak at 400 nm at 1 min and 2 min were used to calculate the Michaelis–Menten constant (K_m).

The solution of AuNP@CDs-Azo-peptide was irradiated with UV (365 nm, 40 mW cm^{-2}) or visible light for 10 min, and then added into the 4-NP solution. A freshly prepared $NaBH_4$ solution was added. The total volume of the solution was 200 μL. The final concentration of 4-NP was 0.075 mM. The absorbance of 4-NP was recorded by UV-Vis spectroscopy (UV-2600, Shimadzu) to calculate the reaction rate constant (k).

Results and discussion

AuNP@CDs and Azo-peptide with different amino acid sequences form three peptide–nanoparticle conjugates through host–guest interactions. The catalytic site is the imidazole group of histidine in the peptide.[16] Due to the different positions of the imidazole group, we speculate that the catalytic performances of the three conjugates for 4-NPA hydrolysis are different. As a control, 4-NPA does not self-hydrolyze in water, and the three peptides do not catalyze 4-NPA hydrolysis. In the presence of peptide–nanoparticle conjugates, 4-NPA will be hydrolyzed to 4-NP (Fig. 1a). The hydrolysis of 4-NPA to 4-NP can be observed with the naked eye. The color of the solution changes from colorless to yellow. 4-NP has a characteristic absorption peak at 400 nm in the UV-Vis spectra. The absorbance at 400 nm was substituted into the standard curve to calculate the concentration of 4-NP. The difference between the concentration of 4-NP in the initial 1 min and 2 min was converted to the initial rate (r_0) that was substituted into the Michaelis–Menten equation $\left(r_0 = \frac{r_{max}[S]}{K_m + [S]}\right)$ to calculate the maximum rate (r_{max}) and the Michaelis–Menten constant (K_m), where [S] is the concentration of the substrate. The linear regression coefficient of the double reciprocal plot is better than that of the r_0-[S] plot. Therefore, peptide–nanoparticle conjugates are a kind of nanozyme,[17–19] a term used to define nanomaterials with enzyme-like properties.[20–25] AuNP@CDs-Azo-HGFGLEK had the highest r_{max} and K_m (Fig. 1b), indicating that it has the lowest affinity for the substrate. This result is not surprising, as the closer the histidine bound to the substrate is to the surface of the nanoparticles, the stronger the steric hindrance effect.[26]

The concentration of 4-NPA at time t obtained by subtracting 4-NPA hydrolysis consumption from the initial concentration was substituted into the integral rate equation $\left(\ln\frac{c_t}{c_0} = -kt\right)$ of the first order reaction to obtain the reaction rate constant (k) by linear fitting. The three nanozymes show good catalytic activity for 4-NPA hydrolysis (Fig. 1c). AuNP@CDs-Azo-HGFGLEK is the best catalyst. The reaction

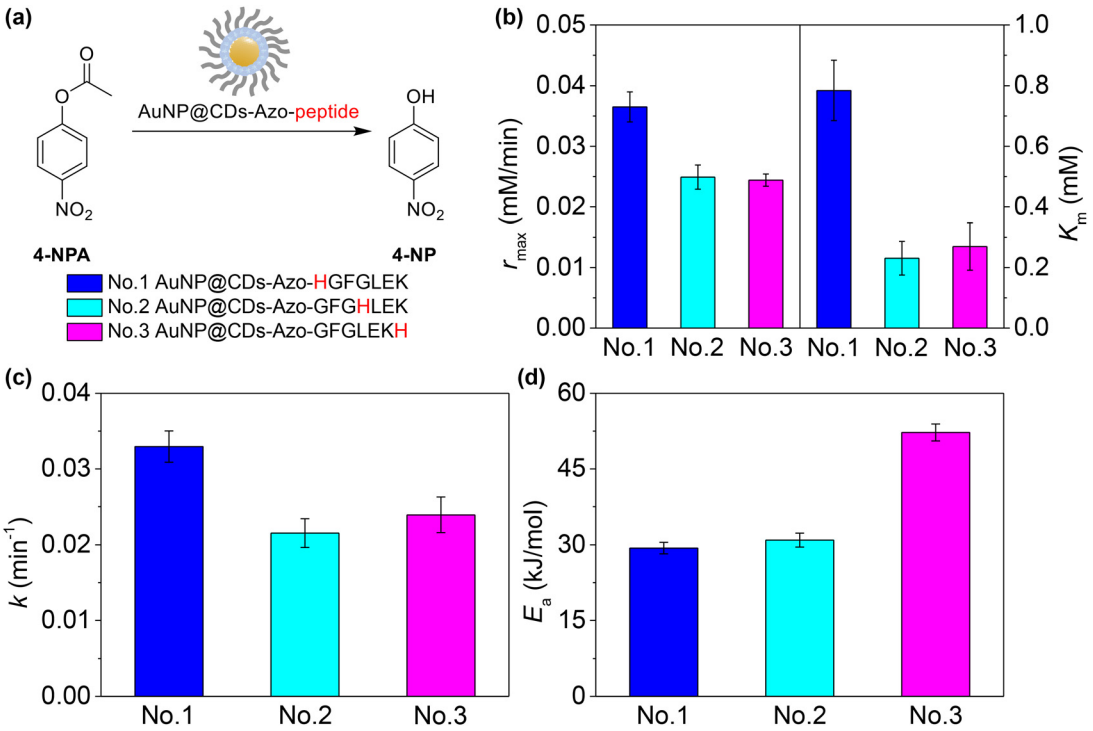

Fig. 1 Biomimetic hydrolysis of 4-NPA by AuNP@CDs-Azo-peptide. (a) Schematic of 4-NPA hydrolysis. (b) Maximum rate (r_{max}) and Michaelis–Menten constant (K_m) calculated according to the Michaelis–Menten equation. (c) Reaction rate constant (k). (d) Activation energy (E_a).

rate constants (k) of catalytic hydrolysis at different temperatures were substituted into the Arrhenius equation $\left(\ln\{K\} = -\frac{E_a}{RT} + \ln\{K_0\}\right)$ to calculate the activation energy (E_a), where R = 8.314 J mol^{-1} K^{-1} (gas constant), T = 300 K (room temperature) and k_0 is the preexponential factor. The E_a of AuNP@CDs-Azo-HGFGLEK for 4-NPA hydrolysis is the lowest (Fig. 1d). On the basis of the results, it can be found that the amino acid sequence is very important for peptide–nanoparticle conjugates. There are reports that the catalytic activity of peptide–nanoparticle conjugates can be regulated by a conformational change and artificial carbonic anhydrase mimics are developed by the addition of Zn(II)-ions to peptide–nanoparticle conjugates.[27,28] Our study shows that the amino acid sequence can not only change the affinity of the peptide to the substrate, but also tune the catalytic activity of the peptide–nanoparticle conjugates. The neighboring histidine in AuNP@CDs-Azo-HGFGLEK is rather close, which helps the proton split from water, thus promoting the nucleophilic attack on the substrate.

Azobenzene has unique a photoresponse (Fig. 2a). Under UV irradiation, azobenzene will change from a *trans*-configuration to a *cis*-configuration. Under visible light irradiation or heat, azobenzene will recover from the *cis*-configuration to the *trans*-configuration. The photoisomerization of azobenzene is reversible.[29] The absorption spectra of *trans*-azobenzene and *cis*-azobenzene are obviously different, so the photoisomerization of azobenzene can be detected by UV-Vis spectroscopy. After irradiating the solution with 365 nm UV light, the absorbance at 324 nm decreases rapidly (Fig. 2b). After 10 min of irradiation, the absorbance no longer decreases. Subsequently, with visible light irradiation, the absorbance at 324 nm of solution increases, and it reaches the equilibrium after 6 min.

Due to the photoisomerization of azobenzene, the disassembly/assembly of AuNP@CDs-Azo-HGFGLEK is regulated by UV/visible light irradiation (Fig. 2c). *Trans*-azobenzene is inserted into the hydrophobic cavity of cyclodextrin on the surface of AuNP@CDs through host–guest interactions. Under UV irradiation, *cis*-azobenzene will break away from the cavity of cyclodextrin due to the change of polarity and molecular size, leading to the destruction of the assembly structure of nanozymes and the decrease of hydrolase-like activity. Under alternative UV/visible light irradiation, hydrolase-like activity is reversibly regulated (Fig. 2d). This reversible process can be repeated many times. The conversion of *cis*-azobenzene to *trans*-azobenzene is not complete, so the catalytic activity of nanozymes will relatively decrease after cyclic irradiation.

AuNP@CDs-Azo-HGFGLEK catalyzes the hydrolysis of 4-NPA to 4-NP. Under UV irradiation, AuNP@CDs-Azo-HGFGLEK disassembles to AuNP@CDs and Azo-HGFGLEK. AuNP@CDs further catalyzes the reduction of 4-NP to 4-AP in the presence of $NaBH_4$ (Fig. 2e). As a control, the catalytic ability of nanozymes for 4-NP reduction is weak without UV irradiation (Fig. 2f). Therefore, it is expected that in one solution, the two-step reaction of the substrate can be completed

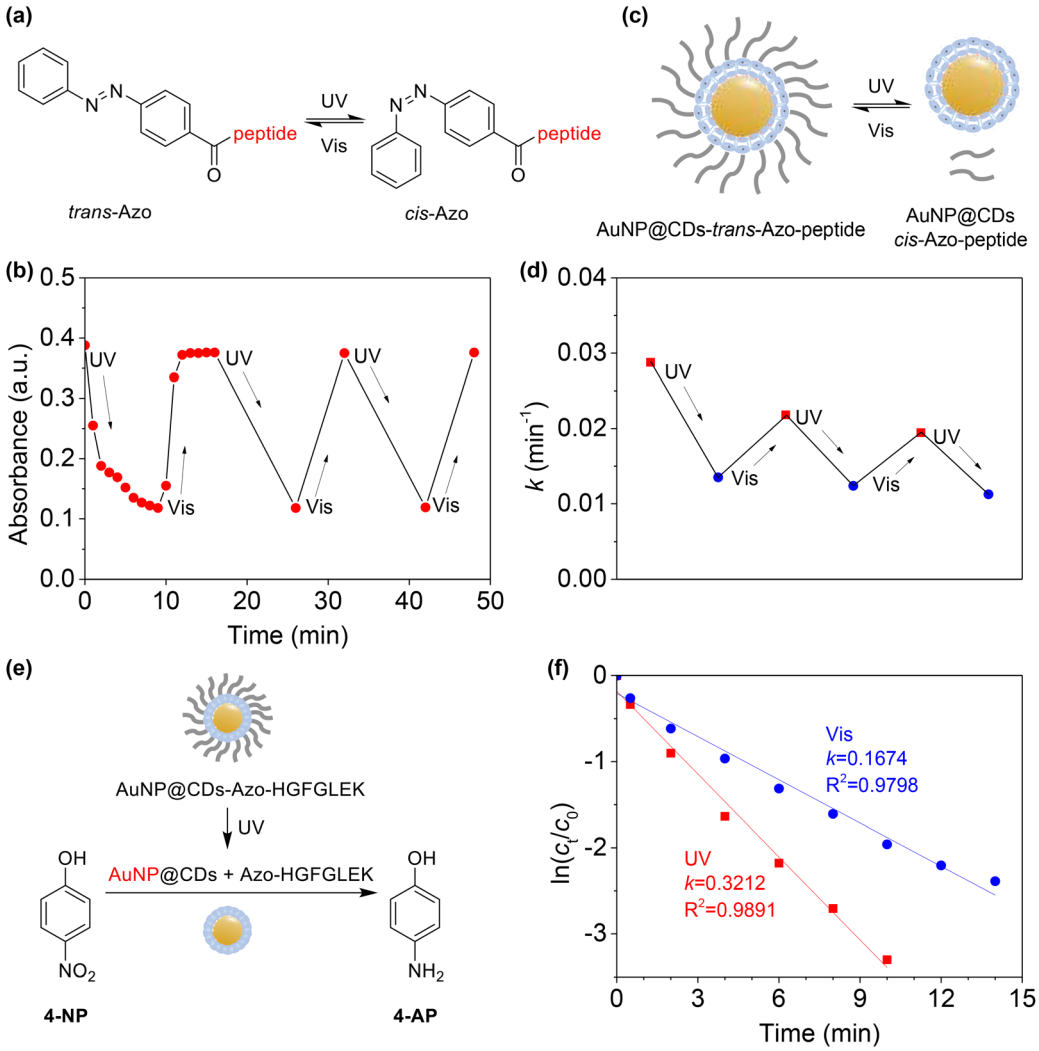

Fig. 2 Photo-regulated catalytic activity of AuNP@CDs-Azo-peptide. (a) Reversible photoisomerization of Azo-peptide. (b) Absorbance of Azo-HGFGLEK with UV/visible light irradiation. (c) Schematic of disassembly/assembly of AuNP@CDs-Azo-peptide with UV/visible light irradiation. (d) Reaction rate constant (k) of AuNP@CDs-Azo-HGFGLEK with UV/visible light irradiation. (e) Schematic of 4-NP reduction. (f) Relationship of $\ln(c_t/c_0)$ and time of 4-NP reduction.

by photoregulation to achieve cascade catalysis (the hydrolysis of 4-NPA to 4-NP and the reduction of 4-NP to 4-AP).[30,31]

Conclusions

AuNP@CDs and Azo-peptide self-assemble through host–guest interactions to form AuNP@CDs-Azo-peptide that is a kind of nanozyme with hydrolase-like activity. The catalytic ability of nanozymes derives from the imidazole group of histidine in the peptide, but the position of the imidazole group is different, which leads to the different catalytic performance of the nanozymes. Our strategy provides an interesting approach to tune the catalytic activity of nanozymes by amino acid sequences. Due to the photoisomerization of azobenzene, AuNP@CDs-Azo-peptide diassembles/assembles and its hydrolase-like catalytic performance is regulated by UV/visible light irradiation. AuNP@CDs-Azo-peptide catalyzes the hydrolysis of 4-NPA to 4-NP, and AuNP@CDs catalyze the reduction of 4-NP to 4-AP. Therefore, it is expected to realize photo-controlled cascade catalysis.

Author contributions

Xiaojin Zhang: investigation and writing – review & editing; Yichuan Wang: formal analysis and investigation; Fan Xia: project administration; Yu Dai: conceptualization, investigation, writing – review & editing, and supervision.

Conflicts of interest

There are no conflicts to declare.

Acknowledgements

This work was financially supported by the Natural Science Foundation of Hubei Province (2022CFB050 and 2020CFA037), National Natural Science Foundation of China (22090050), National Key R&D Program of China (2021YFA1200403), Joint NSFC-ISF Research Grant Program (22161142020), and Zhejiang Provincial Natural Science Foundation of China (LD21B050001).

References

1 P. Makam, S. Yamijala, K. Tao, L. J. W. Shimon, D. S. Eisenberg, M. R. Sawaya, B. M. Wong and E. Gazit, *Nat. Catal.*, 2019, **2**, 977–985.
2 Y. Murakami, J. Kikuchi, Y. Hisaeda and O. Hayashida, *Chem. Rev.*, 1996, **96**, 721–758.
3 E. Kuah, S. Toh, J. Yee, Q. Ma and Z. Q. Gao, *Chem. – Eur. J.*, 2016, **22**, 8404–8430.
4 V. Nanda and R. L. Koder, *Nat. Chem.*, 2010, **2**, 15–24.
5 C. M. Rufo, Y. S. Moroz, O. V. Moroz, J. Stohr, T. A. Smith, X. Z. Hu, W. F. DeGrado and I. V. Korendovych, *Nat. Chem.*, 2014, **6**, 303–309.
6 F. Schneider, *Angew. Chem., Int. Ed. Engl.*, 1978, **17**, 583–592.
7 L. Polgar, *Cell. Mol. Life Sci.*, 2005, **62**, 2161–2172.
8 G. Dodson and A. Wlodawer, *Trends Biochem. Sci.*, 1998, **23**, 347–352.
9 M. O. Guler and S. I. Stupp, *J. Am. Chem. Soc.*, 2007, **129**, 12082–12083.
10 Q. Liu, K. W. Wan, Y. X. Shang, Z. G. Wang, Y. Y. Zhang, L. R. Dai, C. Wang, H. Wang, X. H. Shi, D. S. Liu and B. Q. Ding, *Nat. Mater.*, 2021, **20**, 395–402.
11 Y. A. Zhao, B. Q. Lei, M. F. Wang, S. T. Wu, W. Qi, R. X. Su and Z. M. He, *J. Mater. Chem. B*, 2018, **6**, 2444–2449.
12 S. K. Rout, M. P. Friedmann, R. Riek and J. Greenwald, *Nat. Commun.*, 2018, **9**, 234.
13 Y. C. Wang, Y. F. Han, X. L. Tan, Y. Dai, F. Xia and X. J. Zhang, *J. Mater. Chem. B*, 2021, **9**, 2584–2593.
14 Y. C. Wang, X. J. Zhang, Y. Dai and F. Xia, *Chem. Eng. J.*, 2023, 140811.
15 R. Liu, X. J. Zhang, F. Xia and Y. Dai, *J. Catal.*, 2022, **409**, 33–40.
16 X. J. Zhang, S. J. Lin, Y. C. Wang, F. Xia and Y. Dai, *Chem. Eng. J.*, 2021, **426**, 130855.
17 Y. H. Lin, J. S. Ren and X. G. Qu, *Adv. Mater.*, 2014, **26**, 4200–4217.
18 D. J. Mikolajczak, A. A. Berger and B. Koksch, *Angew. Chem., Int. Ed.*, 2020, **59**, 8776–8785.
19 Q. Hou, X. J. Zhang, M. H. Lin, Y. Dai and F. Xia, *Giant*, 2022, **12**, 100122.
20 H. Wei and E. K. Wang, *Chem. Soc. Rev.*, 2013, **42**, 6060–6093.
21 Y. H. Lin, J. S. Ren and X. G. Qu, *Acc. Chem. Res.*, 2014, **47**, 1097–1105.
22 M. M. Liang and X. Y. Yan, *Acc. Chem. Res.*, 2019, **52**, 2190–2200.
23 J. J. X. Wu, X. Y. Wang, Q. Wang, Z. P. Lou, S. R. Li, Y. Y. Zhu, L. Qin and H. Wei, *Chem. Soc. Rev.*, 2019, **48**, 1004–1076.
24 Y. Y. Huang, J. S. Ren and X. G. Qu, *Chem. Rev.*, 2019, **119**, 4357–4412.
25 X. J. Zhang, S. J. Lin, S. W. Liu, X. L. Tan, Y. Dai and F. Xia, *Coord. Chem. Rev.*, 2021, **429**, 213652.
26 D. J. Mikolajczak, J. Scholz and B. Koksch, *ChemCatChem*, 2018, **10**, 5665–5668.
27 D. J. Mikolajczak, J. L. Heier, B. Schade and B. Koksch, *Biomacromolecules*, 2017, **18**, 3557–3562.
28 D. J. Mikolajczak and B. Koksch, *Catalysts*, 2019, **9**, 903.
29 H. M. D. Bandara and S. C. Burdette, *Chem. Soc. Rev.*, 2012, **41**, 1809–1825.
30 D. J. Mikolajczak and B. Koksch, *ChemCatChem*, 2018, **10**, 4324–4328.
31 X. L. Tan, Y. L. Xu, S. J. Lin, G. F. Dai, X. J. Zhang, F. Xia and Y. Dai, *J. Catal.*, 2021, **402**, 125–129.

